Phase separation in a single-step growth model with surface diffusion

1997 J. Phys. A: Math. Gen. 30 7739

(http://iopscience.iop.org/0305-4470/30/22/013)

J. Phys. A: Math. Gen. **30** (1997) 7739–7752. Printed in the UK PII: S0305-4470(97)84943-8

Phase separation in a single-step growth model with surface diffusion

Joachim Krug†§ and Felix Hontinfinde‡‖

† Fachbereich Physik, Universität GH Essen, D-45117 Essen, Germany

‡ Dipartimento di Fisica, Istituto Nazionale per la Fisica della Materia, Via Dodecaneso 33, 16146 Genova, Italy

Received 12 June 1997

Abstract. We consider a one-dimensional solid-on-solid growth model in which the nearest-neighbour height differences are restricted to take the values ± 1. Deposition occurs at local minima with probability f, while diffusion moves of single adatoms within a layer occur with probability $1-f$. Interlayer transport and detachment from step edges is suppressed. For $f \to 1$ the stationary distribution of the model is known, hence the growth-induced surface current can be computed analytically for small diffusion rates. In the opposite, diffusion-dominated limit, $f \to 0$, a description in terms of step flow is possible for slopes larger than a critical slope u_c. For smaller slopes the surface phase separates into regions of slope $\pm u_c$. The stationary domain size diverges for $f \to 0$ as $f^{-\nu}$, where $\nu \approx 0.5$. We suggest that the large-scale behaviour in this limit can be described by the noisy Kuramoto–Sivashinsky equation in its noise-dominated regime.

1. Introduction

Simple lattice models have played a central role in the development of an improved understanding of far-from-equilibrium crystal growth during the past decade [1–3]. Of particular importance are models which admit at least partial analytic solutions, such as the computation of the exact crystal growth rate in the thermodynamic limit. Several examples for two-and three-dimensional crystals have been constructed by Gates and Westcott (GW) [4, 5]. In these models the kinetic rates for evaporation and condensation of single atoms are prescribed in terms of the local bonding environment, but no mass transport on the surface is allowed for.

In many crystal-growth processes of current interest mass transport through surface diffusion is an essential ingredient, since it provides the efficient microscopic smoothing mechanism required for the growth of atomically flat layers. As was first pointed out by Villain [6], the introduction of surface diffusion induces a wealth of qualitatively novel phenomena, the most prominent of which is a generic growth instability associated with step-edge barriers [7] and corresponding 'uphill' mass currents¶ [8].

It would therefore be most desirable to devise a model for growth with surface diffusion which retains the simple analytic structure of the evaporation–condensation models

§ Corresponding author. E-mail address: jkrug@theo-phys.uni-essen.de

‖ On leave from: LPT-ICAC, Faculté des Sciences, Rabat (Morocco) and IMSP, Université Nationale du Benin, BP 613, Porto-Novo (Benin).

¶ For a review see [3, section 5].

0305-4470/97/227739+14$19.50

introduced by GW [4] and others [9–11]. So far this has proved to be rather difficult. The only known solvable model for growth with surface diffusion refers to a one-dimensional step train in the absence of interlayer transport and in the limit of infinite diffusion length [12], for which the growth-induced surface current [8] can be derived exactly [13, 14].

In a related effort, we have recently extended the GW model to include both in-layer and interlayer surface diffusion [15]. Due to the restriction on the height differences (see section 2) the state space of the model is finite for finite system sizes, and hence the stationary master equation can be solved exactly for small samples. Nevertheless the asymptotic large-scale behaviour is difficult to ascertain from the finite-size results.

In the present paper we simplify the model introduced in [15], reducing the dependence on kinetic barriers and temperature to a single parameter f related to the ratio of diffusion (D) and deposition (F) rates as

$$f = (1 + D/F)^{-1}. \tag{1}$$

We show, through a combination of simulations and analytic arguments, how exact results for the large-scale behaviour of this model can be obtained both in the deposition dominated ($f \to 1$) and the diffusion dominated ($f \to 0$) regimes. The morphological instability typical for growth with surface diffusion is found to persist; however, its character is qualitatively altered due to the fact that the relaxation processes in the model do not conserve the volume of the crystal [16]. Instead of showing domain coarsening [17], the surface phase separates into domains of a *finite* lateral extent $\xi(f)$, which diverges for $f \to 0$ as

$$\xi(f) \sim f^{-\nu} \tag{2}$$

with an exponent $\nu \approx \frac{1}{2}$. We propose a continuum description in terms of a noisy Kuramoto–Sivashinsky equation [18, 19], which suggests that in fact $\nu = \frac{1}{2}$ exactly.

The model of interest is defined in the next section. In section 3 we exploit the knowledge of the trivial stationary distribution of the $f = 1$ model to obtain approximate expressions for the slope-dependent surface current [8] and the adatom density. Section 4 applies previous results for step-flow growth [12–14] to describe tilted surfaces in the regime of small f, and a finite-size scaling analysis of the adatom density is used to extract the domain-size exponent ν in (2). In section 5 our results are put into context and a continuum equation for the model is proposed.

2. Definition of the model

Like the one-dimensional GW model [4], our model can be thought to describe the growing edge of a two-dimensional hexagonal crystal (figure 1). With a suitable choice of units, the one-dimensional surface (shown as a zig-zag line in figure 1) is represented by its integer height h_i above the substrate site i, $i = 1, \ldots, L$. Permitted configurations satisfy the 'single-step' constraint [4, 9–11]

$$\sigma_i \equiv h_{i+1} - h_i = \pm 1 \tag{3}$$

and an average surface tilt,

$$u \equiv \langle \sigma_i \rangle \qquad -1 \leqslant u \leqslant 1 \tag{4}$$

is fixed through helical boundary conditions, $h_{i+L} = h_i + uL$.

In an elementary simulation step a lattice site i is chosen at random, and a *deposition attempt* is made with probability f. Such an attempt is successful only if the chosen site is a local minimum, in the sense that

$$(\sigma_{i-1}, \sigma_i) = (-1, 1) \qquad \text{(deposition site)}. \tag{5}$$

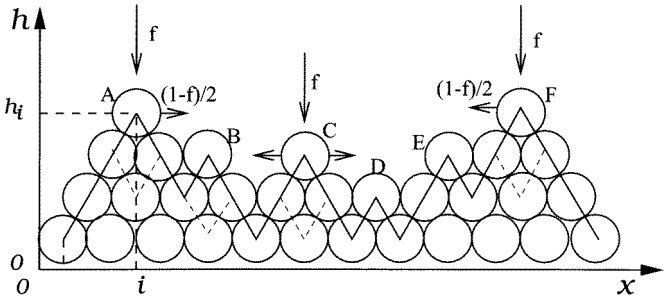

Figure 1. Schematic of the growth model used in this work. The full zig-zag line represents the surface position h_i. Atoms have been deposited at positions A, B, C and F. Prior to deposition a *growth site* (local minimum) existed at these positions, which is indicated by broken lines. Atoms A, C and F are mobile, but only atom C can move in both directions. Atoms A and F give (opposite) contributions to the growth-induced current. Atoms B, D and E are bonded laterally and therefore cannot move.

If the condition (5) is satisfied, the height at site i is increased by two units, $h_i \to h_i + 2$; otherwise the move is discarded, and a new site is chosen.

With probability $1 - f$ a *diffusion attempt* is made instead. This move requires the presence of an isolated adatom at site i, that is, a local slope configuration (see figure 1)

$$(\sigma_{i-2}, \sigma_{i-1}, \sigma_i, \sigma_{i+1}) = (1, 1, -1, -1) \qquad \text{(adatom)}. \tag{6}$$

If such an adatom is found, a decision is made to move it left or right with equal probability. The diffusion move is successful only if, in addition to the condition (6), the neighbouring site which has been chosen is a local minimum and thus can accommodate the adatom. For left (right) moves this implies $\sigma_{i-3} = -1$ ($\sigma_{i+2} = 1$). If one of these additional conditions is violated, the adatom sits at a step edge and therefore is free to move only away from the step (figure 1). In this sense the model includes infinitely strong step-edge barriers [7]; to introduce interlayer transport, diffusion moves to next-nearest neighbour sites would have to be allowed [15]. Related models for surface diffusion without growth have been considered previously by Rácz and coworkers [20].

To make contact with the parameters in more realistic growth models, consider a perfectly 'flat' surface at zero tilt, corresponding to a staggered slope configuration $\sigma_i = (-1)^i$. On such a surface an isolated adatom diffuses with diffusion rate $D = (1-f)/2$, while new atoms are deposited at rate $F = f/2$ per site (every second site is a deposition site (5)). Thus $D/F = (1 - f)/f$ and (1) follows.

We should emphasize that the present model (as well as the one considered in [15]) does *not* belong to the class of 'conserved' growth models [3] of 'ideal' molecular beam epitaxy [16], in which all deposited atoms remain at the surface. The condition (5) on eligible growth sites leads, in effect, to a sticking coefficient which is different from unity [21] and introduces a coupling between the surface morphology and the average growth rate; in particular the growth rate depends on the tilt u for any value of f (see below). It is possible to construct conserved growth models with a 'single step' restriction, but only at the expense of allowing mass transport of unlimited range even in the absence of diffusion. If a particle lands in a large region with no eligible growth sites (e.g. an extended steep hillside), it has to be moved to the edge of that region to be incorporated into the crystal [22, 23]. This introduces long-ranged slope correlations and spoils the simple structure of the stationary distribution [11].

3. Growth-dominated regime: $f \to 1$

In the absence of diffusion ($f = 1$) the stationary state of the infinite system is obtained [9] by choosing the slope variables independently at different sites, with probabilities $(1+u)/2$ for a step up ($\sigma_i = 1$) and $(1-u)/2$ for a step down ($\sigma_i = -1$). The growth rate is then [4, 11, 25]

$$G(u) = \frac{f}{2}(1-u^2) \tag{7}$$

and the probability of finding an adatom configuration (6) is given by

$$\rho_D(u) = \frac{(1-u^2)^2}{16}. \tag{8}$$

Since not all adatoms are actually mobile, a more useful measure of diffusional surface transport is the number of successful diffusion moves per unit time, which is computed, in an obvious notation, as

$$\begin{aligned} n_D(u) &= \frac{1-f}{2}[\mathrm{Prob}(-++--{-}) + \mathrm{Prob}(+++--{+}) + 2\mathrm{Prob}(-++--{+})] \\ &= \frac{1-f}{2}\rho_D(u). \end{aligned} \tag{9}$$

In numerical simulations, the growth-induced surface current $J(u)$ is obtained [8] by recording the difference between left- and right-going diffusion jumps on a tilted surface. For f close to 1 we may use the uncorrelated stationary state to compute the probabilities of various local environments for the diffusing adatom, and hence the net current. The only local configurations which contribute to the current are those where the adatom is located at a descending step edge (figure 1); in all other cases the probabilities of moving left or right are equal. Thus we have

$$\begin{aligned} J(u) &= \tfrac{1}{2}(1-f)[\mathrm{Prob}(+++--{+}) - \mathrm{Prob}(-++--{-})] \\ &= un_D(u) = \frac{(1-f)}{32}u(1-u^2)^2 \end{aligned} \tag{10}$$

where the prefactor $(1-f)/2$ derives from the fact that diffusion moves are attempted with probability $1-f$, and the (allowed) uphill direction is chosen with probability $\frac{1}{2}$. The current is an odd function which vanishes linearly at $u = 0$ and quadratically at $u = \pm 1$, with a maximum at $u = 1/\sqrt{5}$. The simulation data shown in figure 2 confirm that the form of the current is well described by (10) for f close to unity. Moreover, the relation $J(u)/n_D(u) = u$ continues to hold in a range of values of f even when J and n_D are no longer well described by their $f \to 1$ expressions.

While the expressions given above hold in the thermodynamic limit $L \to \infty$, it is a matter of straightforward combinatorics to extend them to finite L. Since quantities like the current (10) probe spatial correlations over extended regions, finite-size effects can be quite prominent.

4. Diffusion-dominated regime: $f \to 0$

4.1. Growth rate

Figure 3 illustrates the change in the tilt-dependent growth rate $G(u)$ as a function of f. For f close to unity one recognizes the familiar parabolic shape of equation (7). Upon

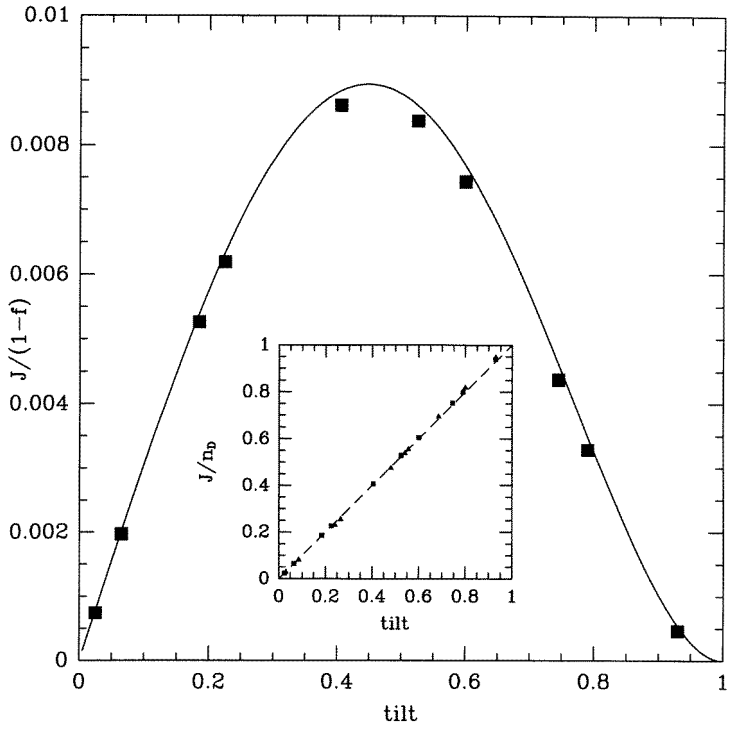

Figure 2. The main figure shows the growth-induced current, normalized by $1-f$, for $f = 0.9$ (full squares) compared with the analytic prediction (10) in the limit $f \to 1$ (full curve). The inset shows numerical data for $f = 0.9$ (full squares) and $f = 0.5$ (full triangles) to illustrate the relation $J/n_D \approx u$. The numerical data were obtained for a system size $L = 400$, and averages were taken over 9×10^6 (5×10^6) monolayers for $f = 0.9$ ($f = 0.5$).

decreasing f the scaled growth rate is seen to approach a *piecewise linear* function,

$$g(u) \equiv \lim_{f\to 0} f^{-1}G(u) = \begin{cases} 1-|u| : |u| > u_c \\ 1-u_c : |u| \leqslant u_c. \end{cases} \tag{11}$$

The critical slope u_c can be estimated rather accurately from a plot of $G(0)/f$ versus f (inset of figure 3), which yields $u_c \approx 0.455$. The deviations from the piecewise linear form visible close to $u = u_c$ for $f \leqslant 0.001$ are presumably finite-size effects. Simulations of smaller systems with $f = 0.01$ showed similar features, which, however, disappeared when the system size was increased. As is detailed in section 4.3, finite-size effects become important when the stationary domain size $\xi(f)$ is comparable with the system size. For $f = 0.001$, the expression (23) yields $\xi \approx 150$, while the system size used in the simulations shown here was only $L = 100$.

Our interpretation of this behaviour is in terms of a transition between two growth regimes occurring at $u = u_c$. For $|u| > u_c$ the surface has the shape of a *step train* (figure 4). In the limit $f \to 0$ this shape is maintained during growth, because each freshly landed particle has enough time to reach a step edge and be absorbed there before the next particle arrives; the corresponding growth mode is referred to as *step flow*. The step train is decomposed into terraces separating single-height or multiple-height steps. Due to the geometry of the model, a terrace consisting of k deposition sites occupies $2k+1$ sites of

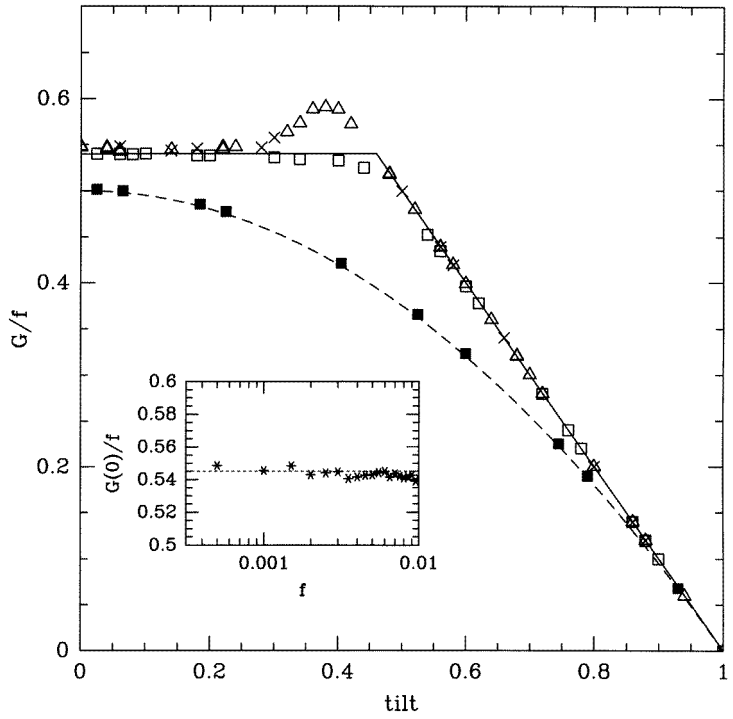

Figure 3. Growth rate, normalized by the deposition rate f, as a function of tilt. The full squares show data for $f = 0.9$, compared with the $f \to 1$ prediction (7) (broken line). Open squares, open triangles and crosses are for $f = 10^{-2}$, $f = 10^{-3}$ and $f = 5 \times 10^{-4}$, respectively. The full curve illustrates the piecewise linear behaviour of equation (11). The data for $f = 0.9$ were obtained by growing 9×10^6 monolayers on a substrate of size $L = 400$. For small values of f the system size used was $L = 100$, and $f \times 10^8$ monolayers were grown for each value of the tilt. The inset shows the normalized growth rate at zero tilt as a function of f. The broken line represents our estimate $G(0) \approx 0.545f$ for $f \to 0$.

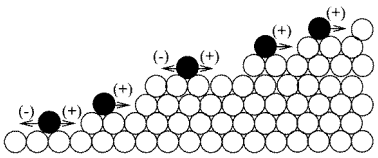

Figure 4. The figure shows a segment of a positively tilted step train. Freshly landed atoms (black) can move uphill (+) or downhill (−) except when they sit at a cliff edge.

the substrate lattice. Consequently the average terrace length for a surface with tilt $u > 0$ is

$$\ell \equiv \langle k \rangle = \frac{1-u}{2u}. \tag{12}$$

The density of deposition sites is then $u\ell = \frac{1}{2}(1-u)$, and since each deposition event increases the height by two units, the growth rate is $f(1-u)$ in accordance with (11).

In the simple square-lattice solid-on-solid model with no interlayer transport the step-flow growth mode has been shown to be unstable due to the nucleation of steep 'towers' of single atoms stacked on top of each other [12]. In the present model the restriction

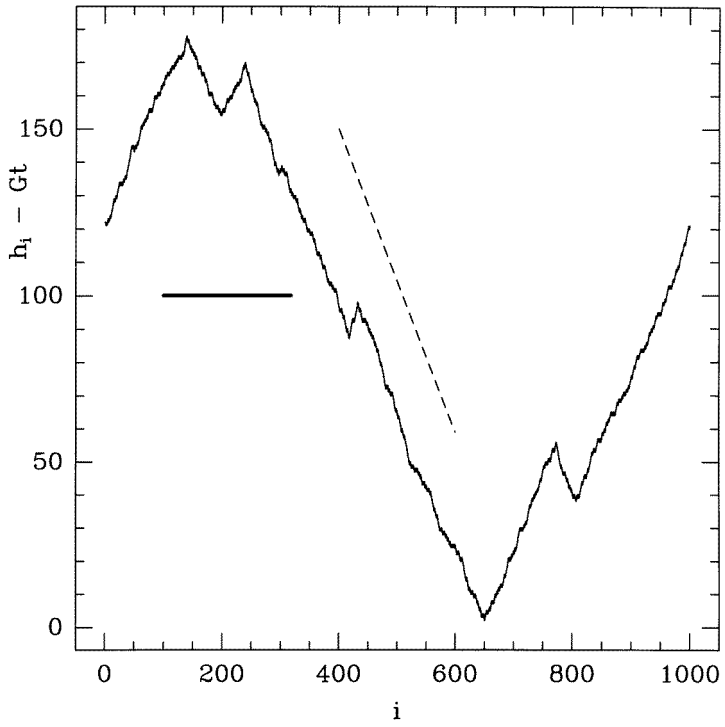

Figure 5. Surface profile for a substrate of zero tilt and size $L = 1000$, onto which 27 250 monolayers have been deposited at a deposition rate $f = 5 \times 10^{-4}$. The heavy bar illustrates the domain size $\xi(f)$ calculated from equation (23), while the broken line indicates the critical slope $u_c \approx 0.455$.

on the height differences appears to stabilize the step train for slopes exceeding u_c. For $|u| < u_c$, the fact that the growth rate becomes independent of tilt indicates that the surface *phase separates* into domains of slopes $\pm u_c$, the fraction of each type of domain being determined by the average slope u. This view is supported by inspection of actual surface profiles (figure 5).

4.2. Surface current

The rescaled surface current also attains a well-defined limiting shape

$$j(u) = \lim_{f \to 0} f^{-1} J(u) \tag{13}$$

for small f (figure 6). To compute the function $j(u)$ in the step-flow regime, we consider an atom deposited onto a terrace of $k > 0$ deposition sites. Let $x = 1, \ldots, k$ denote the deposition site where the atom has landed, with $x = k$ being located next to the ascending step (figure 4). The atom will then have to perform a net number of $k - x$ uphill jumps before being incorporated into the crystal. The average contribution of such an atom to the current is therefore

$$j_k = \frac{1}{k} \sum_{x=1}^{k} k - x = \frac{k-1}{2}. \tag{14}$$

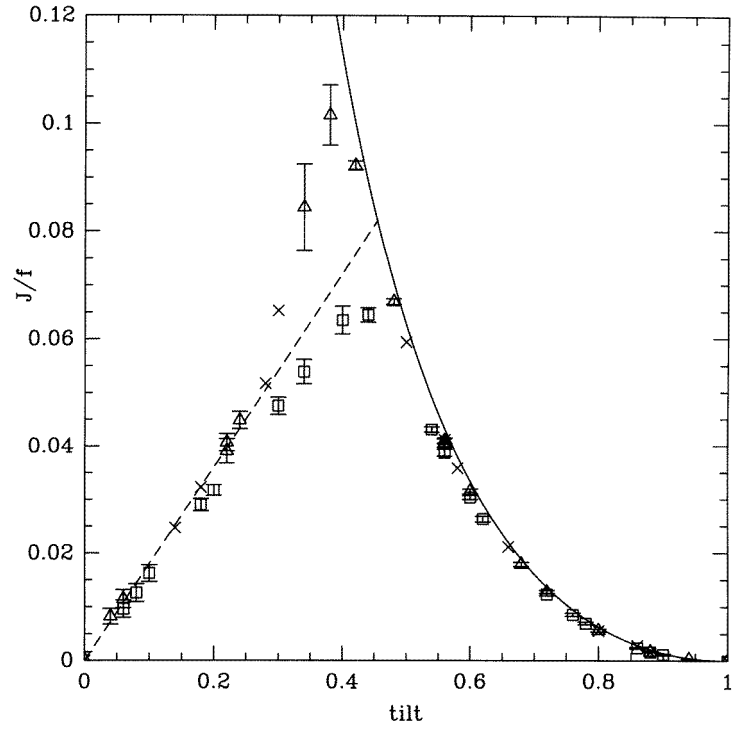

Figure 6. The growth-induced current, normalized by the deposition rate f, as a function of tilt. Parameter values and system sizes associated with the different symbols are the same as in figure 3. The full curve shows the analytic prediction (17) for the step-flow regime, while the broken curve is the linear interpolation (18) of the phase-separated regime. Some representative statistical error bars have been added to illustrate the strong fluctuations near the critical slope.

This has to be averaged with respect to the probability $P(k)$ that a deposited atom lands on a terrace of length k. The terrace lengths for this model can be shown to have a Poisson distribution† [12]. The fact that longer terraces are more likely to capture an atom‡ implies that this distribution has to be multiplied by the terrace length k. The properly normalized expression is therefore

$$P(k) = \frac{k}{\ell}\frac{\mathrm{e}^{-\ell}\ell^k}{k!} \tag{15}$$

and the average migration distance of a deposited atom is obtained as

$$\sum_{k=2}^{\infty} j_k P(k) = \frac{1}{2\ell}\sum_{k=2}^{\infty}\frac{\mathrm{e}^{-\ell}\ell^k}{(k-2)!} = \frac{\ell}{2}. \tag{16}$$

To arrive at the current function $j(u)$ we have to take into account that only a fraction $\frac{1}{2}(1-u)$ of deposition attempts are successful (see section 4.1). The final result therefore reads (using equation (12))

$$j(u) = \frac{1}{4}(1-u)\ell = \frac{1}{8}\frac{(1-u)^2}{u} \tag{17}$$

† The different lattice geometry of the present model does not affect the argument given in [12].

‡ In [14] this effect was overlooked, and it was erroneously concluded that the numerically measured surface current differs from the current function which enters the coarse-grained continuum description of the model.

in excellent agreement with the numerical data in figure 6. Similar expressions have been obtained by Amar and Family [24] for a related model.

In the phase-separated regime $|u| < u_c$ one expects the current to be a linear function of the slope. At an average slope u, a fraction $\frac{1}{2}(1 + u/u_c)$ of the surface has slope u_c, carrying a corresponding current $j(u_c)$, and a fraction $\frac{1}{2}(1 - u/u_c)$ has slope $-u_c$ with the current $-j(u_c)$. The total current is then

$$j(u) = (u/u_c)\, j(u_c). \tag{18}$$

The simulation data are consistent with this picture at least up to $u \approx 0.3$. Closer to the transition the current shows large fluctuations, and presumably also strong finite-size effects (compare with the discussion in section 4.1).

4.3. Adatom density

In this section we consider the frequency of successful diffusion moves n_D, which is a measure of the adatom density (see section 3). As can be seen in the inset of figure 7, in the step-flow regime $n_D(u)$ shows the same kind of scaling as the growth rate and the surface current, in the sense that n_D/f has a well-defined limit for $f \to 0$. This is to be expected, since in the step-flow regime n_D can be written, in analogy to (16), in the form

$$\lim_{f\to 0} n_D/f = \sum_{k=2}^{\infty} n_k P(k) \tag{19}$$

where n_k is the average number of diffusion moves an atom landed on a terrace of size k performs before incorporating at the step edge. Since clearly $n_k \geqslant j_k$ always, it follows that $\lim_{f\to 0} n_D(u)/f \geqslant j(u)$ (see figure 7).

However, the behaviour of n_D in the phase-separated regime $|u| < u_c$ is dramatically different from the quantities G and J considered in the previous two sections. With decreasing tilt, the adatom density rises sharply around $u = u_c$ and saturates to a plateau value which is *not* proportional to f (figure 7). This is due to the appearance of *top terraces* at the local maxima of the surface, where two vicinal facets of tilt $\pm u_c$ meet. The adatom density on the top terraces is much larger than on the vicinal pieces [26], because an atom that is deposited there remains trapped but mobile until a second atom lands with which an island (and therefore a new top terrace) can be formed. It follows that the probability of finding a mobile adatom on a top terrace converges to some finite number for $f \to 0$. The number of top terraces per unit length is proportional to the inverse of the domain size $\xi(f)$ of the faceted pieces. Anticipating the power-law divergence (2) of the domain size for $f \to 0$, it follows that the contribution of the top terraces to the adatom density is of the order f^{ν} and exceeds the contribution $\sim f$ from the vicinal pieces provided $\nu < 1$.

To quantify this picture, we have carried out a finite-size scaling analysis of the stationary value of n_D at zero tilt ($u = 0$) as a function of f and L. For $L \gg \xi$ the adatom density is independent of L and proportional to f^{ν}, while for $L \ll \xi$ there are only two facets, with one top terrace between them, and hence $n_D \sim 1/L$ independent of f. The two regimes are connected by the scaling form

$$n_D(f, L) = L^{-1}\phi(f^{\nu}L) \tag{20}$$

with $\phi(s \to 0) =$ constant, $\phi(s \to \infty) \sim s$. The exponent ν was first estimated using the data for the largest system size $L = 400$ (inset of figure 8), yielding $\nu \approx 0.54$. Then it was verified that this choice also gives an optimal data collapse for all our simulation results, which cover system sizes $20 \leqslant L \leqslant 400$ and deposition rates $5 \times 10^{-4} \leqslant f \leqslant 10^{-2}$.

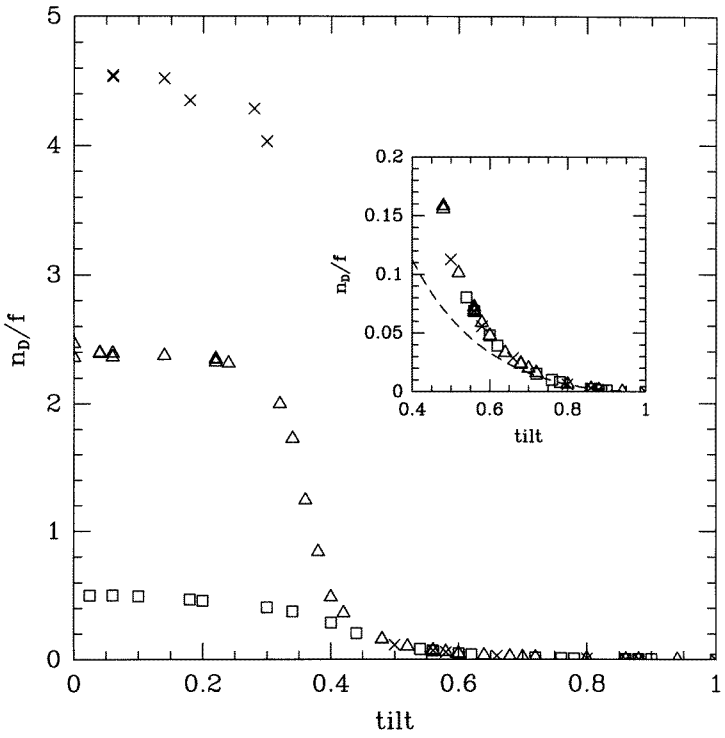

Figure 7. Density of mobile adatoms, normalized by the deposition rate, as a function of tilt. Parameter values and system sizes associated with the different symbols are the same as in figure 3. The inset shows an enlargement of the step-flow regime, to illustrate the date collapse for different f. The broken curve is the expression (17) for the growth-induced current.

Reasonable data collapse was obtained also for $\nu = 0.5$ and $\nu = 0.6$. Thus our subjective best estimate of ν is

$$\nu = 0.54 \pm 0.05 \tag{21}$$

which does not rule out the simple value $\nu = \frac{1}{2}$.

From figure 8 one reads off that the limits of the scaling function ϕ are approximately given by

$$\lim_{s\to 0} \phi(s) \approx 0.20 \qquad \lim_{s\to\infty} \phi(s)/s \approx 0.056. \tag{22}$$

The first estimate implies that the probability of finding a mobile adatom on a top terrace at any given time is about $\frac{1}{5}$. Locating the crossing point s^* between the two asymptotics in equation (22) (figure 8) yields $s^* \approx 3.6$, and hence our numerical estimate for the domain size is

$$\xi(f) \approx 3.6 \times f^{-0.54}. \tag{23}$$

This length scale is indicated as a solid bar in figure 6.

5. Discussion and conclusions

To put our results into perspective, we first briefly review the known theoretical scenarios for unstable epitaxial growth. For models with simple cubic crystal structures and complete

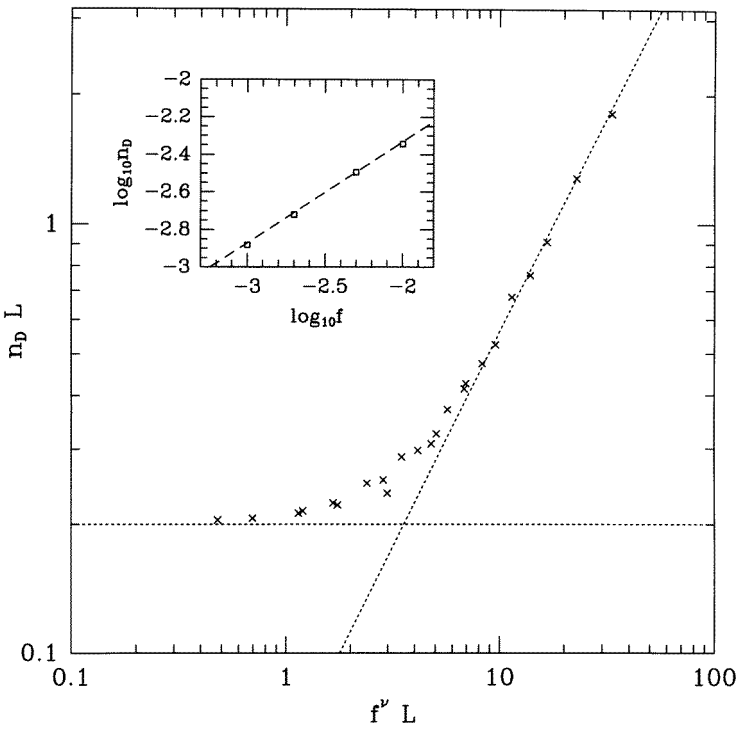

Figure 8. The main figure illustrates the finite-size scaling form (20) for the stationary density of mobile adatoms at zero tilt. The figure shows the optimal data collapse, which was achieved for $\nu = 0.54$. The crosses are simulation data obtained for a variety of system sizes ($20 \leqslant L \leqslant 400$) and deposition rates ($5 \times 10^{-4} \leqslant f \leqslant 10^{-2}$). The number of deposited monolayers ranged from at least 2.5×10^4 for $L = 20$ to 2×10^5 for $L = 400$. The broken lines indicate the limiting behaviours of the scaling function $\phi(s)$ (equation (22)). The inset shows the data for $L = 400$, which were used to estimate ν; the broken line has slope $\nu = 0.54$.

suppression of interlayer transport it is easy to show [12, 13] that the late-stage morphology is completely dominated by the islands formed during the growth in the first layer. The typical feature size ξ is therefore independent of growth time (or coverage), and coincides with the diffusion length ℓ_D of the submonolayer regime. Rate equation theories [27] show that ℓ_D has a power law dependence on the growth parameters,

$$\ell_D \sim (D/F)^\gamma \sim f^{-\gamma} \tag{24}$$

where $\gamma = \frac{1}{4}$ for the case of relevance here (one-dimensional growth with immobile stable dimers).

On the other hand, if some interlayer transport is permitted, the feature size typically increases indefinitely as a power law in time or coverage [17]. The behaviour observed in our model is intermediate between the two cases: a stationary feature size is reached, but, since $\nu \approx \frac{1}{2} > \gamma = \frac{1}{4}$, it is much larger than the submonolayer island size (24). This implies that a certain amount of *coarsening* must take place between the growth of the first layer and the late-stage regime in which ξ saturates. Conversely, since in any case the feature size can only increase with coverage, the argument provides a lower bound $\nu > \gamma = \frac{1}{4}$ on ν. A similar scenario was found by Politi and Villain [26] in a model with *weak* step-edge barriers, where the second length scale fixing the stationary feature size is provided by

barrier strength.

We believe that in our model the stationary domain size originates from the non-conserved character of the dynamics (see section 2), which distinguishes it qualitatively from previous models studied in this context [17, 26]. This issue is most clearly addressed in a continuum language. The standard continuum equation for unstable conserved growth reads [17]

$$\frac{\partial h}{\partial t} + \nabla \cdot (J(\nabla h) + J_{\mathrm{eq}}) = \eta(x,t) \tag{25}$$

where $h(x,t)$ denotes the position of the interface relative to the average, $\eta(x,t)$ is shot noise, J is the growth-induced current [8] and J_{eq} describes smoothing effects. The leading linear terms in a gradient expansion of the current contributions are

$$J \approx -\sigma \nabla h \qquad J_{\mathrm{eq}} \approx \kappa \nabla(\nabla^2 h) \tag{26}$$

where $\kappa > 0$ and $\sigma < 0$ for unstable growth. The balance between the two terms in (26) then defines a length scale ℓ_i associated with the initial stage of the instability,

$$\ell_i \sim \sqrt{\kappa/|\sigma|}. \tag{27}$$

In contrast, the continuum limit of the standard single-step model (our model with $f = 1$) is well known [9, 10, 25] to be the Kardar–Parisi–Zhang (KPZ) equation [1–3, 28]

$$\frac{\partial h}{\partial t} = \sigma \nabla^2 h + \frac{\lambda}{2}(\nabla h)^2 + \eta \tag{28}$$

where [25] $\lambda = 1$ and $\sigma > 0$. The KPZ nonlinearity $(\lambda/2)(\nabla h)^2$ is not allowed in the conserved growth equation (25), but is expected to be present generically in our non-conserved model. The observed phase-separation behaviour for $f \to 0$ indicates that in the diffusion-dominated regime σ becomes negative. Combining equations (25), (26) and (28) we therefore propose that the appropriate continuum equation for small f is the *noisy Kuramoto–Sivashinsky equation* [18, 19]

$$\frac{\partial h}{\partial t} = -|\sigma| \nabla^2 h - \kappa(\nabla^2)^2 h + \frac{\lambda}{2}(\nabla h)^2 + \eta. \tag{29}$$

This equation produces a fluctuating morphology with a typical feature size fixed at ℓ_i. The fluctuations are predominantly of chaotic origin only if the external noise strength is small compared with $|\sigma|^{7/2}$ [3, 19].

To obtain a prediction for the feature size $\xi(f)$ we first recall that the growth-induced current for small f is of the form $J(u) = fj(u)$ (equation (13)), hence $\sigma = -fj'(0)$ and $|\sigma| \sim f$. A number of processes contribute to the coefficient κ of the smoothening current J_{eq} in (26) [29]. In the absence of detachment from step edges, the dominant contribution is expected to be of the form [26, 29]

$$\kappa \sim F \ell_D^4 \sim D f^{1-4\gamma}. \tag{30}$$

From (27) it follows that

$$\xi(f) \sim \ell_i \sim f^{-2\gamma} \tag{31}$$

or $\nu = 2\gamma$. Using the one-dimensional value $\gamma = \frac{1}{4}$ we find $\nu = \frac{1}{2}$, consistent with the numerical results of section 4.3. Moreover, since the noise strength is also proportional to the flux f, and thus much exceeds the chaotic contribution $|\sigma|^{7/2} \sim f^{7/2}$, the model lies in the noise-dominated regime of (29). It is then not surprising that typical configurations (as in figure 5) bear little resemblance to the cellular structures generated by the noiseless

Kuramoto–Sivashinsky equation [18, 19]. Further investigations of the *dynamics* of the model are needed to substantiate this picture.

We conclude with a remark concerning the roughness of the growing surface. For $f = 1$ the stationary surface width is [25]

$$W(L) \equiv \sqrt{\langle (h - \langle h \rangle)^2 \rangle} \approx \sqrt{L/12} \tag{32}$$

for large L. In the phase-separated regime the surface is roof-shaped for $L < \xi(f)$, hence $W \sim L$, which crosses over to $L^{1/2}$ at $L \approx \xi$. Matching the two power laws and using (2) we conclude that

$$W(L) \sim \sqrt{\xi(f)L} \sim f^{-\nu/2} L^{1/2} \tag{33}$$

for $f \ll 1$ and $L \to \infty$. Comparison of (32) with (33) very directly demonstrates the somewhat paradoxical fact that inclusion of surface diffusion in the single-step model *increases* the growth-induced roughness.

A similar conclusion was reached in our earlier work [15]; however, there the technical restriction to small system sizes led to a somewhat different manifestation of the instability. Increasing the temperature, and thus decreasing $F/D \sim f$ at fixed system size induced a transition from the 'rough' regime where $\xi < L$, $W \sim L^{1/2}$, to the 'roof-shaped' regime $\xi > L$, $W \sim L$. Due to the activated temperature dependence of the surface diffusion constant D, the transition appeared to be rather sharp.

Acknowledgments

We acknowledge the kind hospitality of the IFF (Jülich) and the ICTP (Trieste), where most of this work was performed. JK was supported by DFG within SFB 237 *Unordnung und grosse Fluktuationen*.

References

[1] Halpin-Healy T and Zhang Y-C 1995 *Phys. Rep.* **254** 215
[2] Barabási A-L and Stanley H E 1995 *Fractal Concepts in Surface Growth* (Cambridge: Cambridge University Press)
[3] Krug J 1997 *Adv. Phys.* **46** 139
[4] Gates D J and Westcott M 1988 *Proc. R. Soc.* A **416** 443
Gates D J and Westcott M 1988 *Proc. R. Soc.* A **416** 463
Gates D J 1988 *J. Stat. Phys.* **52** 245
Gates D J and Westcott M 1994 *J. Stat. Phys.* **77** 199
[5] Gates D J and Westcott M 1995 *J. Stat. Phys.* **81** 681
Prähofer M and Spohn H 1997 *J. Stat. Phys.* in press
[6] Villain J 1991 *J. Physique* I **1** 19
[7] Schwoebel R L and Shipsey E J 1966 *J. Appl. Phys.* **37** 3682
Ehrlich G and Hudda F G 1966 *J. Chem. Phys.* **44** 1039
[8] Krug J, Plischke M and Siegert M 1993 *Phys. Rev. Lett.* **70** 3271
[9] Meakin P, Ramanlal P, Sander L and Ball R C 1986 *Phys. Rev.* A **34** 5091
Sander L M 1991 *Solids Far From Equilibrium* ed C Godrèche (Cambridge: Cambridge University Press) p 433
[10] Plischke M, Rácz Z and Liu D L 1987 *Phys. Rev.* B **35** 3485
[11] Krug J and Spohn H 1991 *Solids Far From Equilibrium* ed C Godrèche (Cambridge: Cambridge University Press) p 479
[12] Krug J and Schimschak M 1995 *J. Physique* I **5** 1065
[13] Krug J 1997 *J. Stat. Phys.* **87** 505
[14] Krug J 1997 *Dynamics of Fluctuating Interfaces and Related Phenomena* ed D Kim, H Park and B Kahng (Singapore: World Scientific) p 95

[15] Hontinfinde F, Krug J and Touzani M 1997 *Physica* **237A** 363
[16] Lai Z-W and Das Sarma S 1991 *Phys. Rev. Lett.* **66** 2348
[17] Hunt A W, Orme C, Williams D R, Orr B G and Sander L M 1994 *Europhys. Lett.* **27** 611
Siegert M and Plischke M 1994 *Phys. Rev. Lett.* **73** 1517
Siegert M and Plischke M 1996 *Phys. Rev.* E **53** 307
Rost M and Krug J 1997 *Phys. Rev.* E **55** 3952
[18] Kuramoto Y 1984 *Chemical Oscillations, Waves, and Turbulence* (Berlin: Springer)
Sivashinsky G I 1983 *Ann. Rev. Fluid Mech.* **15** 179
[19] Karma A and Misbah C 1993 *Phys. Rev. Lett.* **71** 3810
[20] Rácz Z, Siegert M, Liu D and Plischke M 1991 *Phys. Rev.* A **43** 5275
[21] Kang H C and Evans J W 1992 *Surf. Sci.* **269/270** 784
[22] Meakin P and Jullien R 1987 *J. Physique* **48** 1651
Jullien R and Meakin P 1987 *Europhys. Lett.* **4** 1385
[23] Kim Y, Park D K and Kim J M 1994 *J. Phys. A: Math. Gen.* **27** L533
Kim Y and Kim J-M 1997 *Phys. Rev.* E **55** 3977
[24] Amar J G and Family F 1996 *Phys. Rev.* B **54** 14 071
[25] Krug J, Meakin P and Halpin-Healy T 1992 *Phys. Rev.* A **45** 638
[26] Politi P and Villain J 1996 *Phys. Rev.* B **54** 5114
Politi P 1997 *J. Physique* I **7** 797
[27] Wolf D E 1995 *Scale Invariance, Interfaces and Non-equilibrium Dynamics* ed M Droz, A J McKane, J Vannimenus and D E Wolf (New York: Plenum) p 215
[28] Kardar M, Parisi G and Zhang Y-C 1986 *Phys. Rev. Lett.* **56** 889
[29] Politi P and Villain J 1997 *Surface Diffusion: Atomistic and Collective Processes* ed M Scheffler and M Tringides (New York: Plenum)